The Astrophysical Journal, 964:30 (10pp), 2024 March 20 https://doi.org/10.3847/1538-4357/ad27d9

The Impact of Breathing Pulses during Core Helium Burning on the Core Chemical Structure and Pulsations of Hydrogen-rich Atmosphere White Dwarfs

Alejandro H. Córsico[1,2] and Leandro G. Althaus[1,2]
[1] Grupo de Evolución Estelar y Pulsaciones. Facultad de Ciencias Astronómicas y Geofísicas, Universidad Nacional de La Plata, Paseo del Bosque s/n, (1900) La Plata, Argentina; acorsico@fcaglp.unlp.edu.ar
[2] Instituto de Astrofísica de La Plata, IALP (CCT La Plata), CONICET-UNLP, Argentina
Received 2023 December 18; revised 2024 February 2; accepted 2024 February 3; published 2024 March 13

Abstract

Breathing pulses are mixing episodes that could develop during the core helium-burning phase of low- and intermediate-mass stars. The occurrence of breathing pulses is expected to bear consequences on the formation and evolution of white dwarfs, particularly on the core chemical structure, which can be probed by asteroseismology. We aim to explore the consequences of breathing pulses on the chemical profiles and pulsational properties of variable white dwarf stars with hydrogen-rich envelopes, known as ZZ Ceti stars. We compute stellar models with masses of $1.0M_{\odot}$ and $2.5M_{\odot}$ in the zero-age main sequence and evolve them through the core helium-burning phase to the thermal pulses on the asymptotic giant branch, and finally to advanced stages of white dwarf cooling. We compare the chemical structure of the core of white dwarfs whose progenitors have experienced breathing pulses during the core helium-burning phase with the case in which breathing pulses have not occurred. We find that when breathing pulses occur, the white dwarf cores are larger and the central abundances of oxygen are higher than for the case in which the breathing pulses are suppressed, in line with previous studies. However, the occurrence of breathing pulses is not sufficient to explain the large cores and the excessive oxygen abundances that characterize recently derived asteroseismological models of pulsating white dwarfs. We find absolute differences of up to ∼30 s when we compare pulsation periods of white dwarfs coming from progenitors that have experienced breathing pulses with the case in which the progenitors have not suffered breathing pulses.

Unified Astronomy Thesaurus concepts: Stellar interiors (1606); White dwarf stars (1799)

1. Introduction

White dwarf (WD) stars constitute the final product of the evolution of low- and intermediate-mass stars, that is, stars with initial masses lower than $\sim$10–11$M_{\odot}$, depending on their initial metallicity (Woosley & Heger 2015). Once low- and intermediate-mass stars leave the main sequence, when the central hydrogen (H) content has been exhausted, helium (He) ignites in the central regions, giving rise to the core He-burning (CHeB) phase. During the CHeB stage, the structure of the core of stars is supposed to consist roughly of a central He-burning convection zone that is surrounded by a He-rich region that is not convective. The structure of the edge of the convective core is highly uncertain and has a direct impact on the duration of this phase and the pulsational properties of stars in the CHeB stage (e.g., subdwarf B stars, horizontal branch stars, RR Lyrae stars, and red giant stars), and also on the subsequent evolution. In particular, the treatment of the uncertainties in the mixing of material at the edge of the convective core during the CHeB phase leads to different possible chemical structures of the core of the emerging WDs.

One of the most uncertain aspects of the CHeB phase—that has been (and continues to be) subject of debate—is the possible occurrence of mixing episodes called "breathing pulses" (BPs; Sweigart & Demarque 1973; Castellani et al. 1985) that take place late in the CHeB phase. At this stage, the position of the formal convective boundary becomes unstable to mixing episodes, and BPs may arise as a rapid growth in the mass of the convective core when the central He abundance is very low ($X_{\rm He} \lesssim 0.10$) and the ^{12}C(α, γ)^{16}O reaction dominates on the triple-α reaction. The effect of BPs is to carry fresh He from the nonconvective mantle into the convective core, thus prolonging the CHeB lifetime. As a result of BPs, the mass of the convective core grows significantly, and the central abundance of oxygen (^{16}O) increases (Constantino et al. 2016, 2017). Hence, the occurrence or not of BPs in low- and intermediate-mass stars is expected to bear consequences on the formation and evolution of WDs, in particular their core chemical structure. BPs should not be confused with the "thermal pulses" (TPs) that take place late in the asymptotic giant branch (AGB) evolution. They are distinct phenomena in the context of stellar evolution. TPs typically refer to episodic events during the AGB phase, characterized by a sudden increase in the rate of He burning in the shell surrounding the stellar core. This results in a temporary expansion of the outer envelope and an increase in luminosity (see, for instance, Kippenhahn et al. 2013).

The structure and chemical constituents of the inner cores of WDs—besides other important properties such as stellar mass, rotation, etc.—can be assessed through asteroseismology, a modern approach based on the comparison of the observed oscillation periods of pulsating WDs with theoretical periods calculated on appropriate stellar models (Fontaine & Brassard 2008; Winget & Kepler 2008; Althaus et al. 2010b; Córsico et al. 2019). Recent asteroseismological studies of pulsating DA (H-rich atmospheres) WDs—also called DAV or ZZ Ceti stars—and pulsating DB (He-rich atmospheres) WDs—also known as DBV or V777 Her stars—based on static parametric models of WDs have been carried out by Giammichele et al. (2018, 2021) and Charpinet et al. (2021). In the case of four DAV

stars (SDSS J1136+0409, EPIC 220347759, KIC 11911480, and L 19−2), and a DBV star (KIC 08626021), these studies have resulted in asteroseismic models characterized by cores and central O abundances that are substantially larger than those predicted by canonical evolutionary calculations of WD progenitors (Althaus et al. 2010a; Renedo et al. 2010; Salaris et al. 2010; Althaus & Córsico 2022). In this sense, Timmes et al. (2018) have shown that the inclusion of neutrino cooling in the models of DB WDs could lead to a different asteroseismological model for KIC 08626021 than the one found by Giammichele et al. (2018). However, the inclusion of this effect by Charpinet et al. (2019) seems to lead to a seismological model for this star that is qualitatively similar to that originally found by Giammichele et al. (2018). De Gerónimo et al. (2019) explored in detail the possible changes in the $C^{12}(\alpha, \gamma)^{16}O$ reaction rate, screening processes, microscopic diffusion, and overshooting efficiency during CHeB that could lead to a chemical structure similar to that found by Giammichele et al. (2018) for a DBV star such as KIC 08626021 through asteroseismology. They found that within the current understanding of WD formation from single-star evolution, it is virtually impossible to reproduce the most important asteroseismologically derived features of the chemical structure of KIC 08626021. An additional criticism of Giammichele et al. (2018) results comes from the analysis of Bell (2022), who has shown that the asteroseismic radius determination reported by these authors for KIC 08626021 is 6σ discrepant with constraints from Gaia astrometry, calling into question the other results of that asteroseismic analysis, especially the high (central) O abundance that stellar evolutionary models are not able to reproduce.

The larger cores and central O abundances reported by Giammichele et al. (2018, 2021) and Charpinet et al. (2021) have raised the question of whether it is possible that such chemical structures of the WD cores may certainly be the result of physical processes during the evolution of the progenitor stars. Recently, Giammichele et al. (2022) have proposed a plausible explanation for the large cores with high central O abundances characterizing the asteroseismological models of some pulsating WD stars, as being due to the fact that BPs do take place during the CHeB phase of the WD progenitors. However, the occurrence of BP during the CHeB phase is at odds with the observed ratio of AGB to horizontal branch stars in globular clusters and with asteroseismological inferences in red clump stars in the Kepler field (Constantino et al. 2016, 2017). Given the intriguing suggestion proposed by Giammichele et al. (2022), which, at the same time, generates controversy concerning star counts in globular clusters and the peak of the luminosity distribution function, a thorough exploration of this concept is warranted.

In this work, we examine the chemical structure of the core of WDs whose progenitors have experienced BPs during the CHeB phase and compare it to the case in which BPs have not occurred. We will specifically concentrate on the case of DA WDs; however, the conclusions drawn from our analysis also hold true for DB WDs resulting from isolated evolution. We explore the mass range of interest for ZZ Ceti stars. In addition, we study the impact of the occurrence of BPs on the g-mode period spectrum of WD models representative of ZZ Ceti stars. The paper is organized as follows. In Section 2 we describe the evolutionary computations of WDs from the zero-age main sequence (ZAMS) taking into account and neglecting BPs. In Section 3 we analyze the chemical structure of our resulting WD models. We devote Section 4 to describing our analysis of the impact of core BPs experienced by WD progenitors on the period spectrum of ZZ Ceti models. Finally, in Section 5 we summarize our findings.

Table 1
Basic Model Properties for Our Sequences

$M_{\rm ZAMS}$ ($M_\odot$)	$M_{\rm WD}$ ($M_\odot$)	$\log M_{\rm H}$ ($M_\odot$)	$t_{\rm CHeB}$ (Myr)	$X_{^{16}\rm O}$	$N_{\rm TP}$	$N_{\rm BP}$	C/O
			BP				
1.0	0.5363	−3.612	130.4	0.808	4	5	0.29
2.5	0.5903	−4.149	177.3	0.804	12	3	2.31
			Non-BP				
1.0	0.5343	−3.595	108.2	0.724	4	0	0.29
2.5	0.5868	−4.147	157.1	0.749	13	0	2.48

Note. $M_{\rm ZAMS}$: initial mass; $M_{\rm WD}$: WD mass; $\log M_{\rm H}$: logarithm of the mass of H left in the star at the maximum effective temperature at the beginning of the cooling branch; $t_{\rm CHeB}$: lifetime during CHeB phase; $X_{^{16}\rm O}$: central oxygen abundance; $N_{\rm TP}$: number of thermal pulses; $N_{\rm BP}$: number of BP pulses; C/O: surface carbon (^{12}C) to ^{16}O ratio after departure from the AGB.

2. Evolutionary Computations and Treatment of Breathing Pulses

We have considered two sets of evolutionary sequences. In one of these sets, the occurrence of BPs during the CHeB phase has been considered ("BP case"). In the other set, BPs have been neglected ("non-BP case"). All of the sequences were computed for metallicity $Z = 0.01$ starting from the ZAMS and evolved through the CHeB phase to the thermal pulses on the AGB and finally to the domain of the ZZ Ceti stars at advanced stages of WD cooling. For this purpose, we have used the stellar evolution code LPCODE, developed by the La Plata group (Althaus et al. 2005; Salaris et al. 2013; Althaus et al. 2015; Miller Bertolami 2016; Althaus & Córsico 2022). Our treatment for the progenitor evolution considers new observational constraints and recent advances in the micro- and macrophysics involved in the modeling of CHeB, AGB, and thermally pulsing phases (see Miller Bertolami 2016 for details). We focus our study on average-mass ($0.53 \lesssim M_\star/M_\odot \lesssim 0.60$) pulsating WDs resulting from the single evolution of low-mass progenitors. In particular, we consider WD progenitors of initial mass $M_\star = 1.0$ and $2.5 M_\odot$.

The evolutionary history of progenitor stars determines the internal chemical profile of the WDs, and thus their pulsational properties. This is particularly relevant concerning the evolutionary stages corresponding to the CHeB phase. In order for our models to experience core BPs during this phase, we closely follow the mixing scheme presented in Constantino et al. (2016, 2017). To this end, we adopt their standard-overshoot model, which naturally leads to the occurrence of BPs. Here, time-dependent overshoot mixing is implemented with an exponential decay in the diffusion coefficient $D_{\rm OV}$ beyond all convective boundaries according to $D_{\rm OV} = D_{\rm C} \exp(-2z/H_{\rm v})$ where $D_{\rm C}$ is the diffusion coefficient at the edge of the convection zone, and z is the radial distance from the boundary of the convection zone, $H_{\rm v} = fH_P$, where the free parameter f is a measure of the extent of the overshoot region, and H_P is the pressure scale height at the convective boundary. In this study, we have adopted $f = 0.005$ for the CHeB phase. At this value, our code predicts the maximum CHeB lifetimes and central oxygen abundances. Non-BP sequences were computed following the same scheme as described. However,

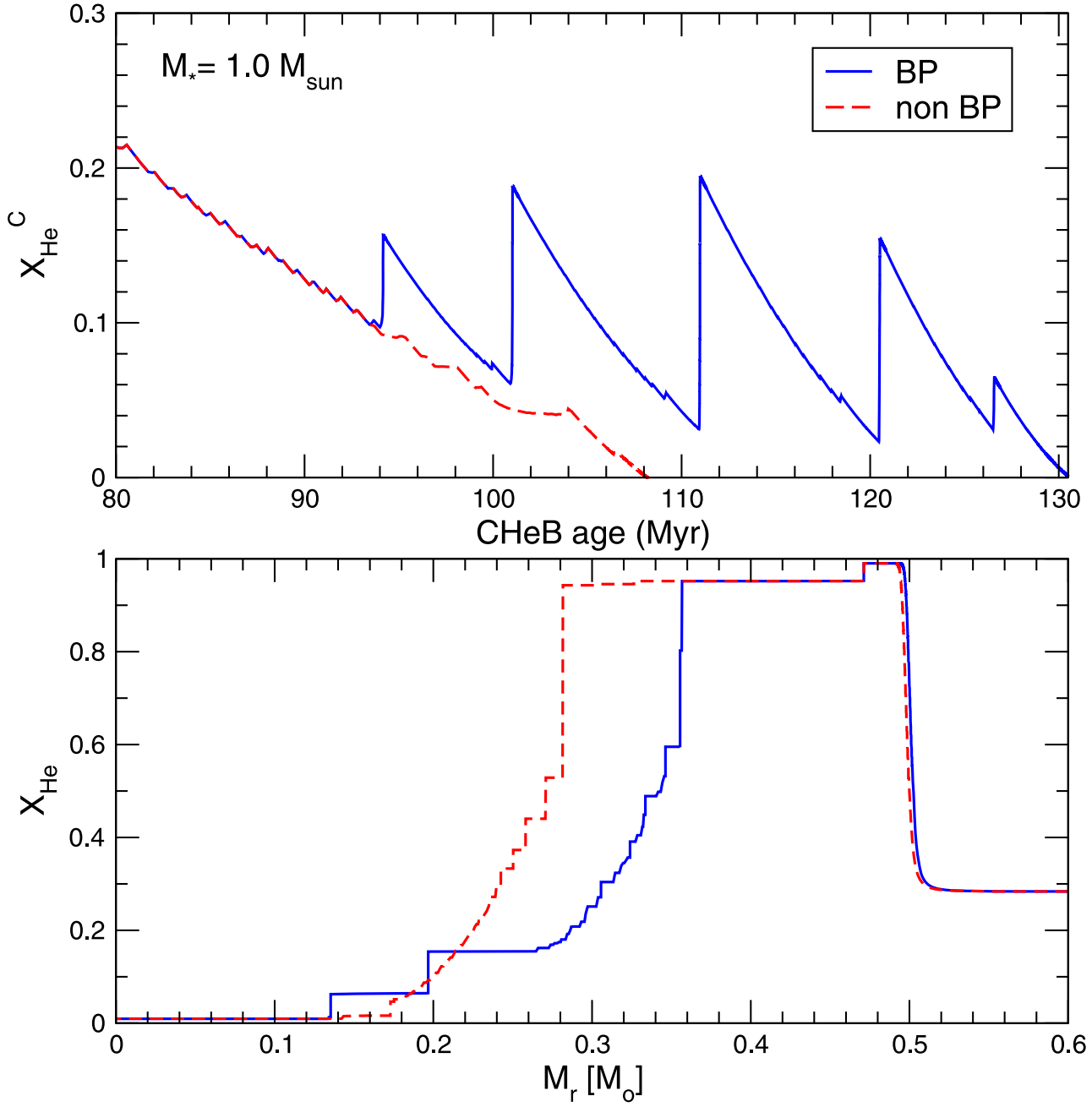

Figure 1. Upper panel: core He abundance (by mass) in terms of the CHeB age. The solid (dashed) line corresponds to the case in which BPs during the CHeB phase have been allowed (suppressed). Bottom panel: inner He abundance distribution at the end of the CHeB phase when the central He abundance is $X_{\rm He} \approx 0.01$ for the two situations illustrated in the upper panel.

in contrast to Constantino et al. (2016, 2017) who employed the formulation by Spruit (2015), we have simply inhibited the BPs by halting the enlargement of the convective core whenever it would result in an increase of the central He abundance. In both cases (BP and non-BP sequences), and in agreement with Constantino et al. (2016, 2017), we find that our sequences develop a large partially mixed region with a stepped composition profile around the convective core. We mention that in all of our calculations, the Schwarzschild criterion for convection is used. In Table 1 we list some relevant quantities of our sequences.

Figure 1 (see also Table 1) clearly shows that the occurrence of BPs extends the lifetime of the CHeB phase as a result of the larger amount of He burned during this phase, as compared with the situation in which BPs are suppressed. This shortens the lifetime of the following early AGB phase because of the less amount of available He that is left for this phase, as shown in the bottom panel of Figure 1. This figure depicts the results for our 1.0 $M_{\odot}$ evolutionary sequence and are in line with the findings of Constantino et al. (2016, 2017). The less amount of He that is left for the AGB phase as a result of the occurrence of BPs has no appreciable impact on the emerging WD. In particular, only minor differences are expected in the final H content and stellar mass of the WD, and in the third dredge-up episodes (as reflected by the final surface ^{12}C–^{16}O ratio) that take place during the thermally pulsing AGB phase of WD progenitor. However, as we will see, the chemical structure of the core is substantially affected by the occurrence of BPs

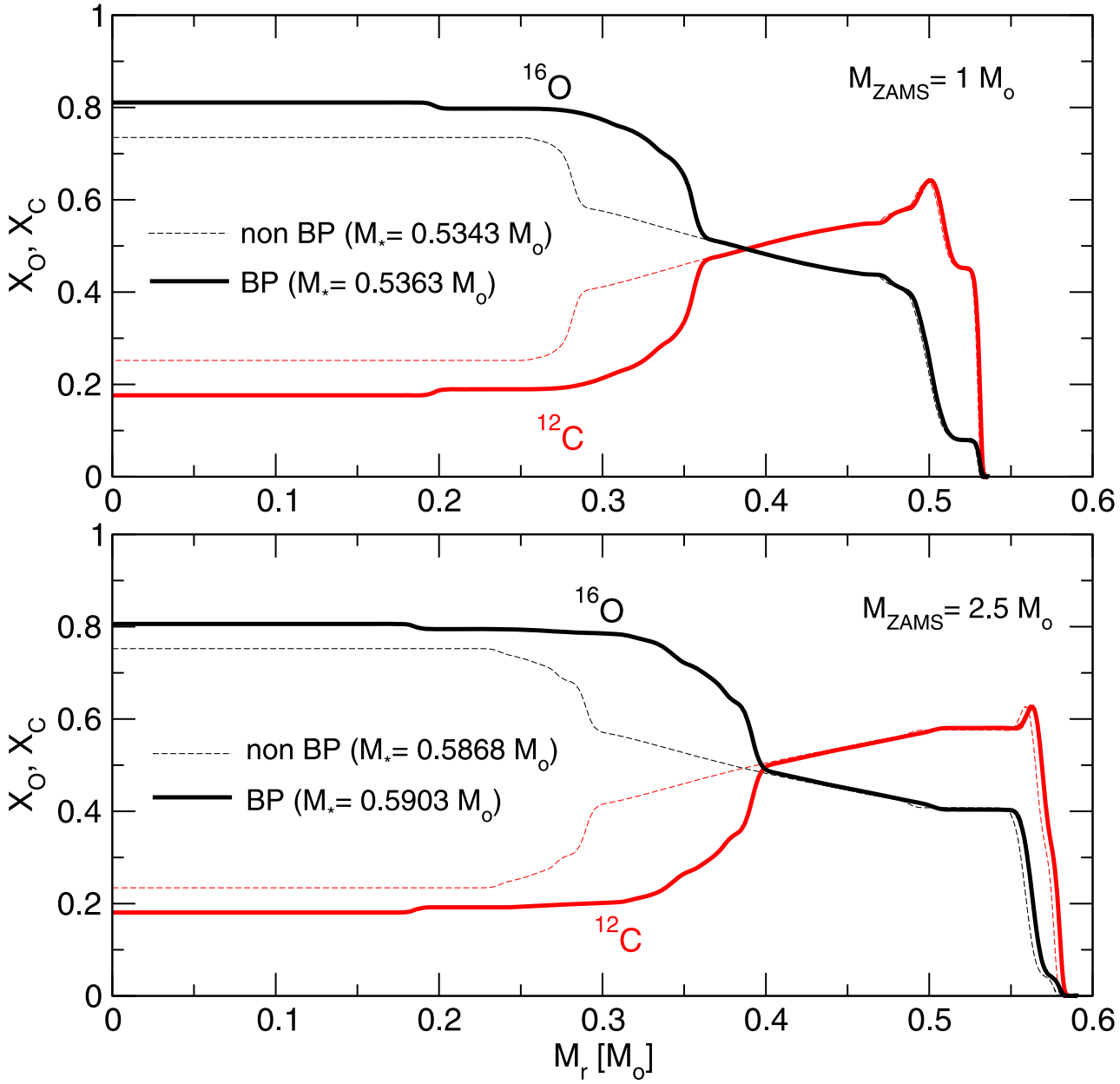

Figure 2. Chemical profiles of ^{16}O (black) and ^{12}C (red) in terms of the mass coordinate (in solar mass units), corresponding to template WD models with $T_{\rm eff} = 12,400$ K. Thin dashed (thick solid) lines correspond to the case in which BPs during the CHeB evolution of the WD progenitor have been suppressed (allowed to occur). The upper panel corresponds to $M_\star = 0.5343 M_\odot$ (non-BP case) and $M_\star = 0.5363 M_\odot$ (BP case), whereas the lower panel corresponds to $M_\star = 0.5868 M_\odot$ (non-BP case) and $M_\star = 0.5903 M_\odot$ (BP case).

during the CHeB phase. This behavior is also essentially the same for the $2.5 M_\odot$ evolutionary sequence studied in this work.

3. Chemical Profiles

We show in the upper panel of Figure 2 the ^{16}O and ^{12}C chemical profiles (fractional mass abundances) as a function of the mass coordinate (in units of solar masses) for two template WD models at $T_{\rm eff} = 12,400$ K, extracted from the $1.0 M_\odot$ WD progenitor evolution for the BP and non-BP cases (thick and thin lines, respectively). The model corresponding to the non-BP case has a stellar mass of $M_\star = 0.5343 M_\odot$, and the model of the BP case is characterized by $M_\star = 0.5363 M_\odot$. The model that has experienced BPs exhibits a higher central abundance of ^{16}O than the model that has not experienced BPs in the previous evolutionary history ($X_{^{16}\rm O} = 0.808$ versus $X_{^{16}\rm O} = 0.724$). A second relevant feature that can be seen in the figure is the larger size of the core for the BP case. Indeed, the total ^{16}O content ($M_{^{16}\rm O}$) in the BP case is $0.66 M_\star$, and for the non-BP case $0.60 M_\star$. In the lower panel, we show the chemical profiles for the case of two template models extracted from the $2.5 M_\odot$ WD progenitor evolution for the BP and non-BP cases (thick and thin lines, respectively). The results for these more massive models are qualitatively similar to those described before for the less massive model, that is, in the case in which BPs are allowed, the core is larger and the central abundance of ^{16}O is higher than for the case in which the BPs are suppressed.

These results were expected, and are in qualitative agreement with previous works (e.g., Constantino et al. 2016, 2017). In particular, we obtain results also in line with the computations

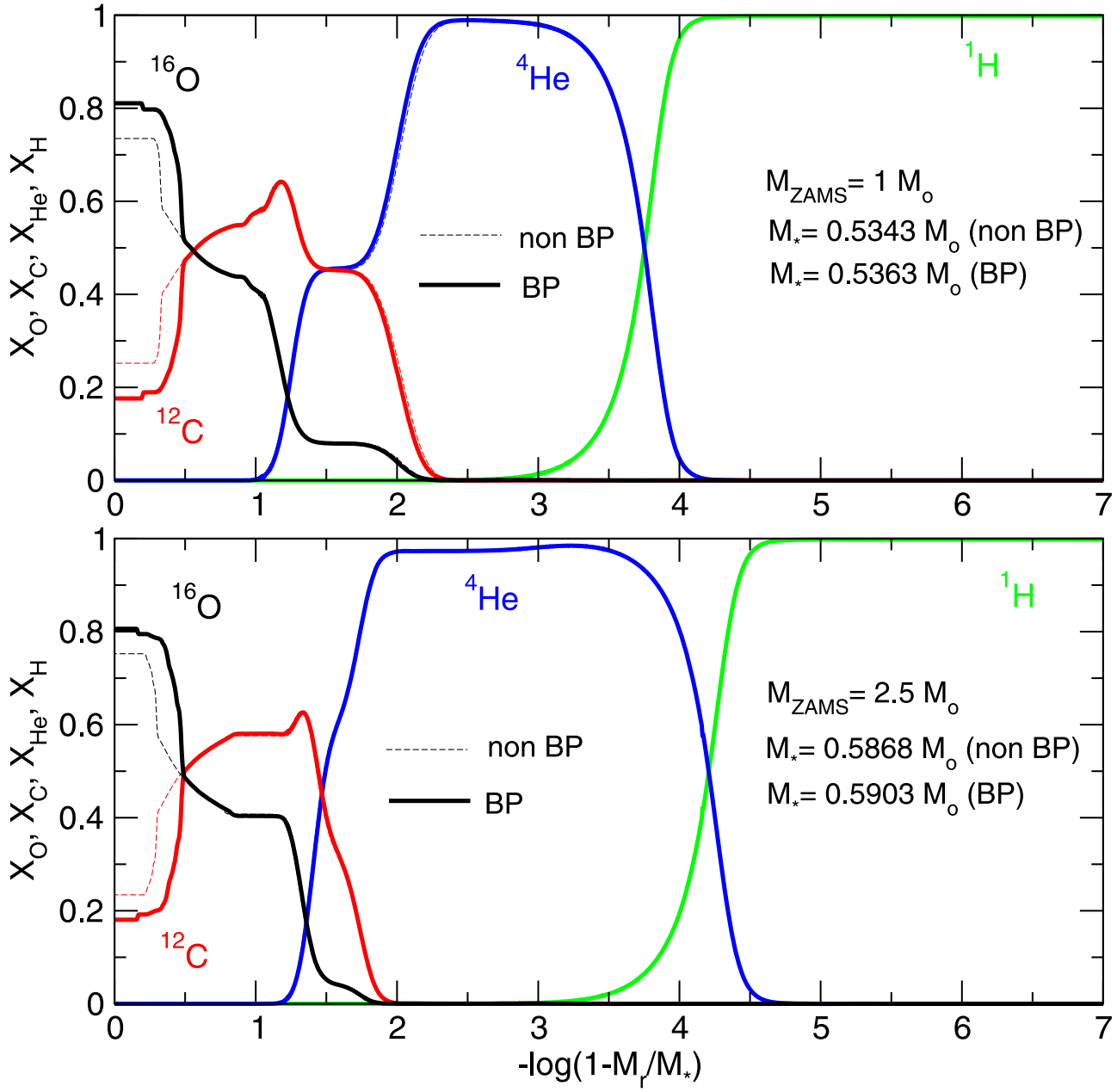

Figure 3. Chemical profiles of ^{16}O (black), ^{12}C (red), ^{4}He (blue), and ^{1}H (green) in terms of outer mass fraction coordinate corresponding to the same template WD models with $T_{\rm eff}$ = 12, 400 K shown in Figure 2. Again, thin dashed lines correspond to the non-BP case, while solid thick lines correspond to the BP case.

of Giammichele et al. (2022), who obtain more massive WD cores with larger central abundances of ^{16}O when taking into account the occurrence of BPs. Nevertheless, we cannot help but notice that we are not able to obtain such a high central abundance of ^{16}O as they derive ($X_{^{16}O} = 0.86$) when considering BPs. Our results considering the occurrence of BPs neither explain the high central ^{16}O abundance nor the huge ^{16}O content of the core asteroseismologically derived by Giammichele et al. (2018) for the DBV star KIC 08626021, of $X_{^{16}O} = 0.86$ and $M_{^{16}O} = 0.78 M_*$, respectively.

It should be noted that the evolutionary calculations of Giammichele et al. (2022) do not include the AGB phase, but are restricted to producing extreme horizontal branch models and evolving them through the He-core- and He-shell-burning phases, and then letting them contract and cool on the WD sequence. Since our simulations include the complete evolution from the ZAMS through the AGB phase to the WD stage, our analysis is able to account for all the processes that ultimately shape the WD internal chemical stratification from the center to the surface. We depict in Figure 3 the complete chemical structure of the species ^{16}O, ^{12}C, ^{4}He, and ^{1}H of the same template WDs models presented in Figure 2, as a function of the logarithm of the outer mass fraction. The imprints of the occurrence of thermal pulses during progenitor evolution manifest themselves as the presence of the intershell rich in helium, carbon, and oxygen, as illustrated in the upper panel of Figure 2. This intershell is not present in the WD models resulting from the more massive progenitor (see bottom panel) because in this case, element diffusion turns out to be much more efficient in shaping the final chemical structure of the intershell by the time the ZZ Ceti domain is reached. Apart from the differences in the size of the core and in the central

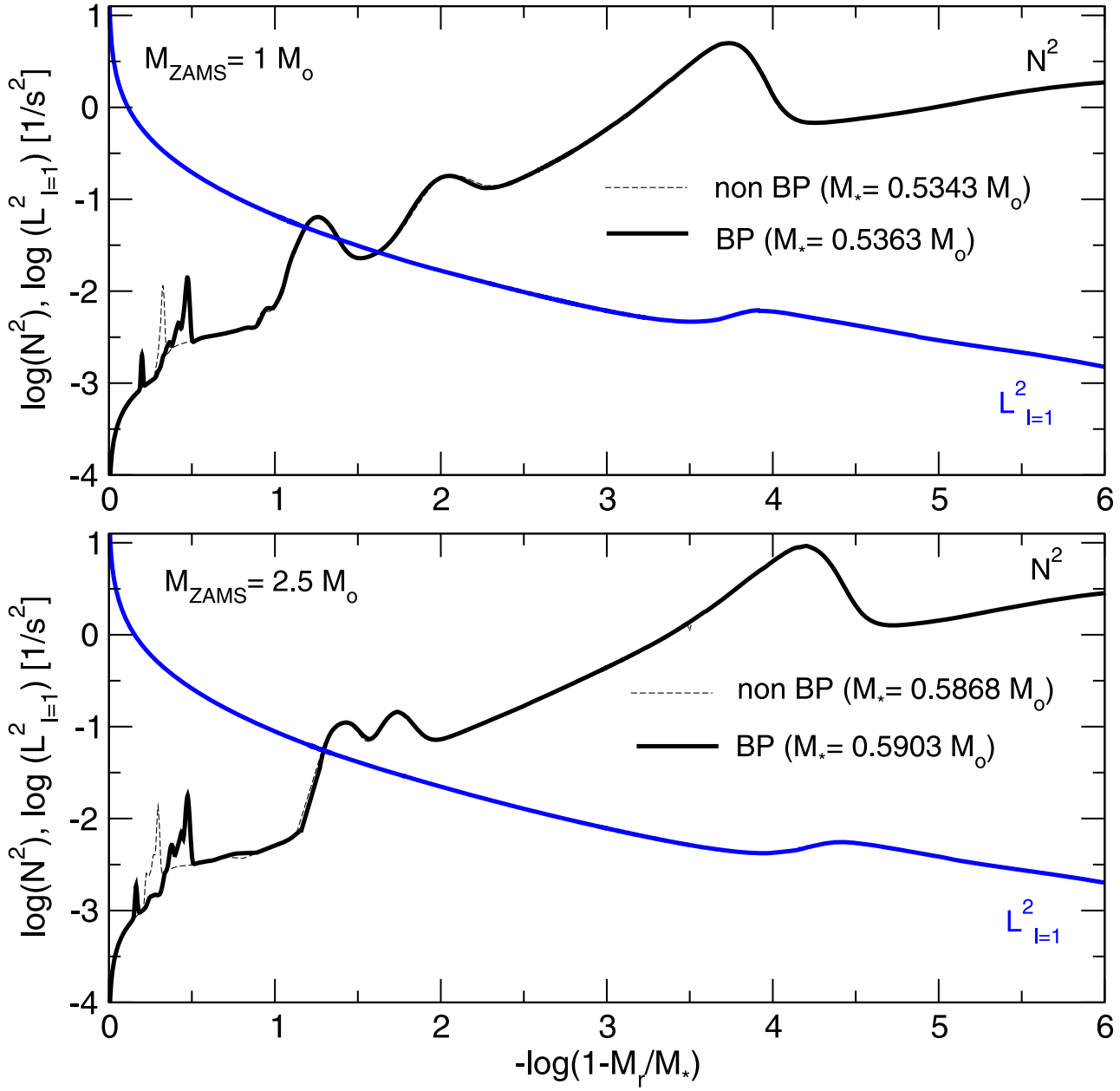

Figure 4. Logarithm of the squared Brunt–Väisälä (black) and Lamb (blue) critical frequencies for $\ell = 1$ modes in terms of the outer mass fraction coordinate, corresponding to the same template WD models with $T_{\rm eff} = 12,400$ K depicted in Figures 2 and 3. Thin dashed (thick solid) lines correspond to the non-BP case (BP case).

abundance of ^{16}O already displayed in Figure 2, this plot shows that there are no appreciable differences in the chemical profiles in other parts of the models, resulting from the occurrence of BPs. The differences in the core chemical structure have consequences on the period spectrum of the WDs. We focus on this issue in the next section.

4. Pulsations

We assess the impact of BPs during the CHeB phase on the pulsation spectrum of WDs by comparing the g-mode period spectrum of models that were computed in the non-BP case and models constructed in the BP case. The pulsation modes of our DA WD models have been computed with the adiabatic version of the `LP-PUL` pulsation code described in Córsico & Althaus (2006).

The squared Brunt–Väisälä frequency (N, the critical frequency of nonradial g-mode pulsations) is computed as in Tassoul et al. (1990), according to the following expression:

$$N^2 = \frac{g^2\rho}{P}\frac{\chi_{\rm T}}{\chi_\rho}[\nabla_{\rm ad} - \nabla + B], \tag{1}$$

where g, ρ, P, $\nabla_{\rm ad}$, and ∇ are the acceleration of gravity, density, pressure, adiabatic temperature gradient, and actual temperature gradient, respectively. The compressibilities χ_ρ and $\chi_{\rm T}$ are defined as

$$\chi_\rho = \left(\frac{d\ln P}{d\ln\rho}\right)_{{\rm T},\{{\rm X}_i\}} \qquad \chi_{\rm T} = \left(\frac{d\ln P}{d\ln T}\right)_{\rho,\{{\rm X}_i\}}. \tag{2}$$

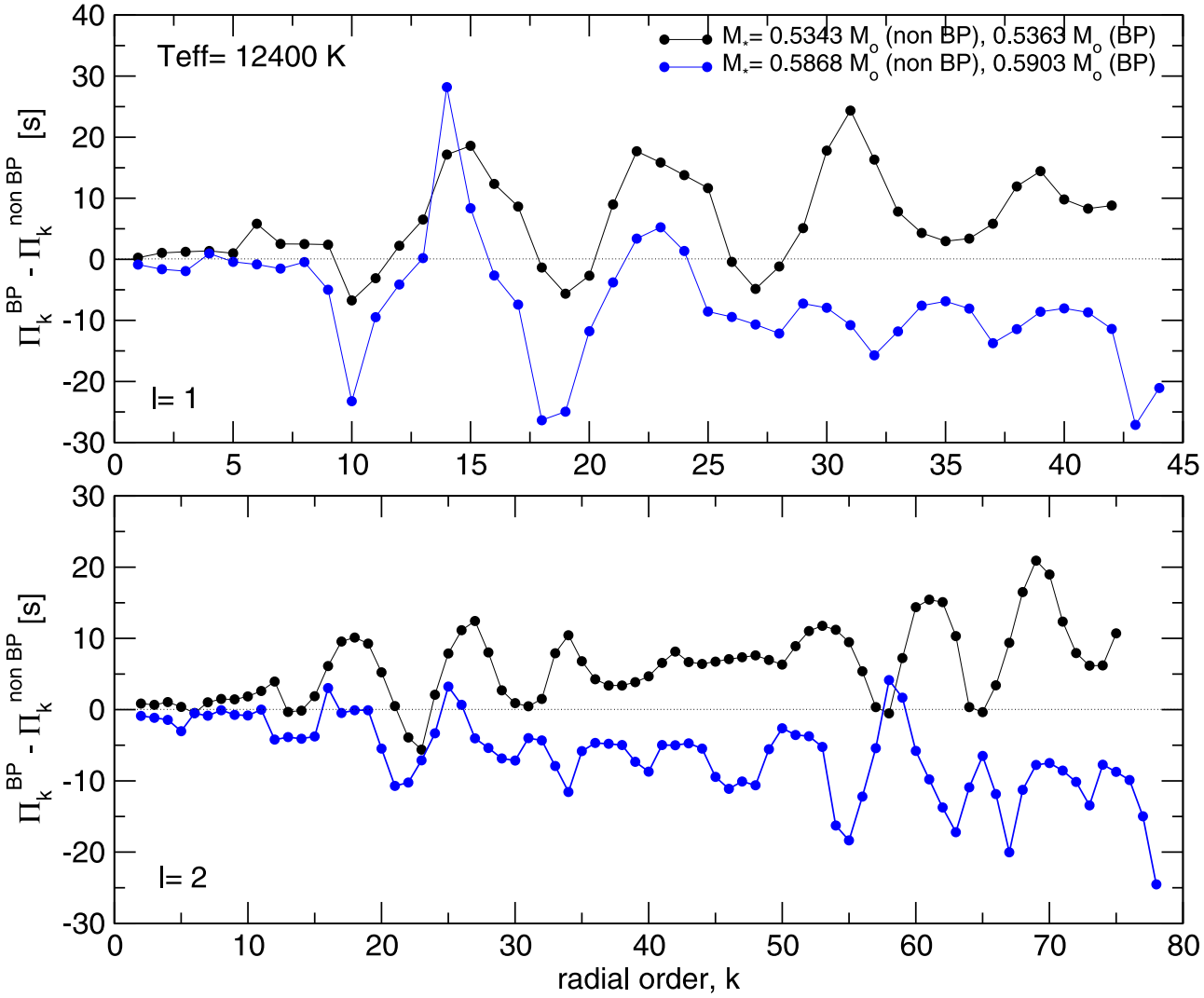

Figure 5. Period differences (with fixed radial order k) in terms of k between the BP and non-BP template models with $T_{\rm eff} = 12,\,400$ K and stellar masses $M_\star \sim 0.53 M_\odot$ ($M_{\rm ZAMS} = 1.0 M_\odot$; black) and $M_\star \sim 0.59 M_\odot$ ($M_{\rm ZAMS} = 2.5 M_\odot$; blue), corresponding to $\ell = 1$ (upper panel) and $\ell = 2$ (lower panel) modes.

Finally, the Ledoux term B is computed as (Tassoul et al. 1990)

$$B = -\frac{1}{\chi_{\rm T}} \sum_{1}^{M-1} \chi_{{\rm X}_i} \frac{d \ln X_i}{d \ln P}, \tag{3}$$

where

$$\chi_{{\rm X}_i} = \left(\frac{d \ln P}{d \ln X_i} \right)_{\rho,{\rm T},\{{\rm X}_{j \neq i}\}}. \tag{4}$$

The computation of the Ledoux term includes the effects of an arbitrary number of chemical species that vary in abundance in the transition regions. For completeness, we also calculate the Lamb frequency (L_ℓ, the critical frequency of nonradial p-mode pulsations) according to the expression

$$L_\ell^2 = \ell(\ell+1) \frac{c_{\rm s}^2}{r^2}, \tag{5}$$

where $c_{\rm s}$ is the local velocity of sound.

The run of the logarithm of the squared Brunt–Väisälä and Lamb ($\ell = 1$) frequencies for the same template models displayed in Figures 2 and 3 are shown in the two panels of Figure 4. As can be seen in the figure, all the bumps of the Brunt–Väisälä frequency are located at the same places within the models, except in the case of the C/O chemical transition at the core. Indeed, the main peak of N^2 at the core of the BP case models is located further out than in the non-BP case models. Additionally, in the BP case models, there exists an additional peak located in deeper regions of the core. This last peak is due to the small step exhibited by the ^{16}O and ^{12}C profiles at $-\log(1 - M_r/M_\star) \sim 0.2$ (see Figure 3).

The differences in the spatial location and number of bumps in the profile of N^2 at the core of the template WD models have sizeable consequences on the pulsation periods and period spacings of the g modes. For the case of individual periods, this is evident in Figure 5, in which we have plotted the difference between the dipole ($\ell = 1$) and quadrupole ($\ell = 2$) periods of g modes calculated in the BP case ($\Pi_k^{\rm BP}$) and the periods calculated in the non-BP case ($\Pi_k^{\rm non-BP}$) in terms of the radial order k, for the same template WD models considered in the previous figures. As can be seen, the absolute value of the difference in the periods can reach up to $\sim$30 s for modes with periods in the range 100–2000 s, the period interval in which the periods observed in ZZ Ceti stars generally fall. The differences in the periods come almost exclusively from the different chemical structures of the core of the WDs depending

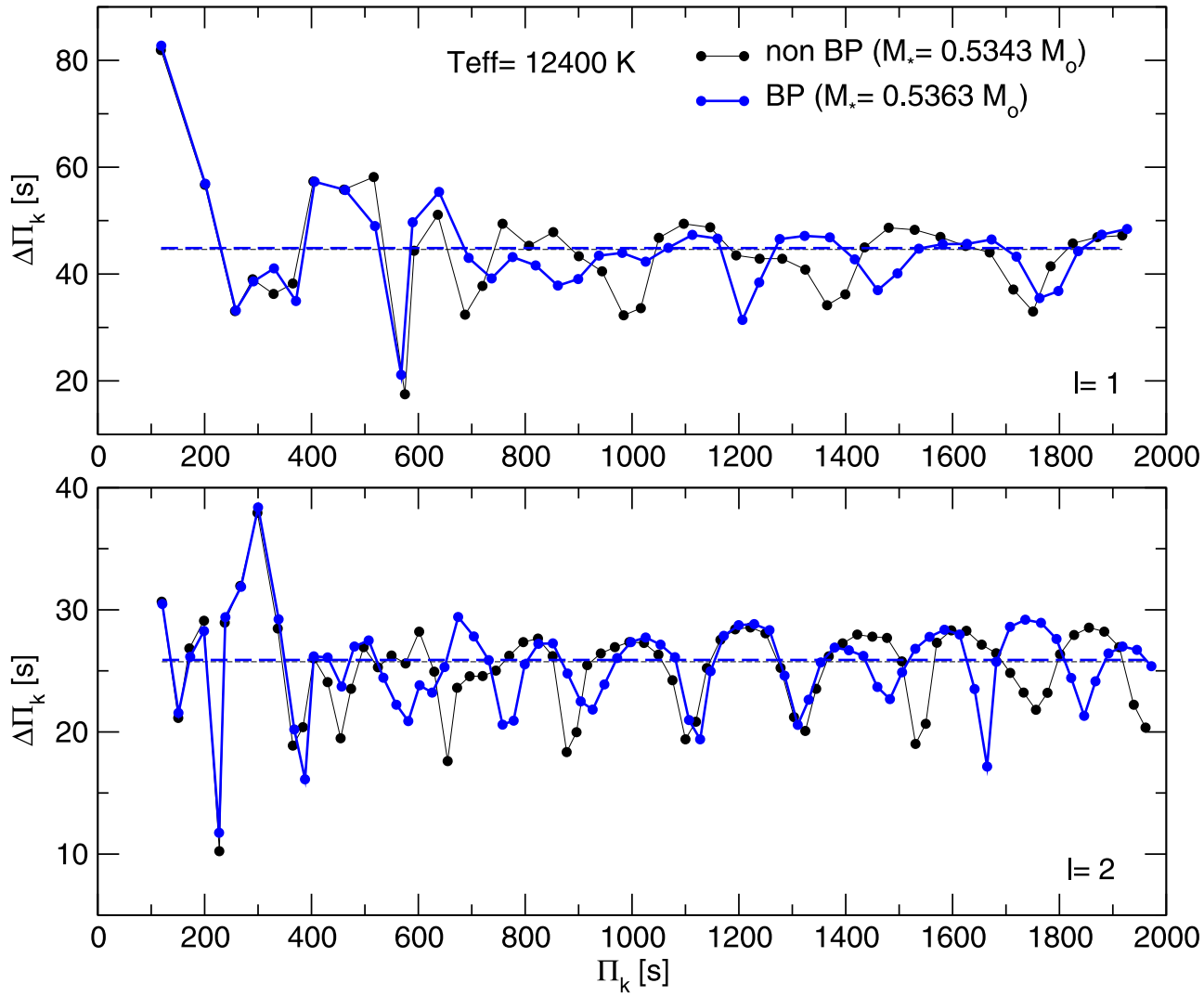

Figure 6. Forward period spacings vs. periods for $\ell = 1$ (upper panel) and $\ell = 2$ (lower panel) g modes, corresponding to the DA WD template models with $T_{\rm eff} = 12,400$ K representative of ZZ Ceti stars. Black (blue) dots connected with black thin (blue thick) lines correspond to the non-BP (BP) case for a ZZ Ceti model with $M_\star = 0.5343 M_\odot$ ($M_\star = 0.5343 M_\odot$).

on the case (BP and non-BP). The tiny difference in mass ($|\Delta M_\star| = |M_\star^{\rm BP} - M_\star^{\rm non-BP}| \lesssim 0.0035 M_\odot$) between the couples of template models has a negligible impact on the periods.

In closing, we depict in Figures 6 and 7 the forward period spacing, defined as $\Delta\Pi_k \equiv \Pi_{k+1} - \Pi_k$, in terms of periods ($\Pi_k$), for dipole (upper panel) and quarupole (lower panel) modes corresponding to the case in which BPs have been considered (blue symbols and thick lines) and the situation in which BPs have been suppressed (black symbols and thin lines) during the CHeB phase. As can be seen, the general appearance of the period-spacing distribution is similar for the BP and the non-BP cases, but there are substantial quantitative differences for periods longer than $\sim$400 s. The asymptotic period spacing (horizontal dashed lines) is slightly different between both cases due to the small difference in stellar mass of the models of the non-BP and BP cases. We conclude that the mean period spacing of pulsating DA WDs is insensitive to the occurrence or not of BPs. However, seismological period-to-period fits of ZZ Ceti stars based on evolutionary models generated considering and neglecting the occurrence of BPs during CHeB could help shed some light on the occurrence of BPs in nature.

5. Summary and Conclusions

In this work, we have revisited the issue of BPs, which consist of mixing events that can occur at the end of the CHeB phase during the evolution of low- and intermediate-mass stars (Sweigart & Demarque 1973; Castellani et al. 1985). The occurrence or not of BPs is expected to have an influence on the evolution of WDs, in particular on their core chemical structure, which can be probed through asteroseismology. Interestingly enough, recent studies of pulsating WDs (Giammichele et al. 2018; Charpinet et al. 2021; Giammichele et al. 2021) point to asteroseismological models characterized by central ^{16}O abundances and core sizes significantly larger than standard WD formation theory indicates. This has given rise to the belief that the cores of WDs in general should be larger and more ^{16}O-rich than previously believed, suggesting that some piece of physics in the formation of WDs has been missing until now (Giammichele et al. 2018). In particular, Giammichele et al. (2022) have claimed that a possible explanation for these anomalous properties of the WD cores could be at the root of the BP episodes during the CHeB phase.

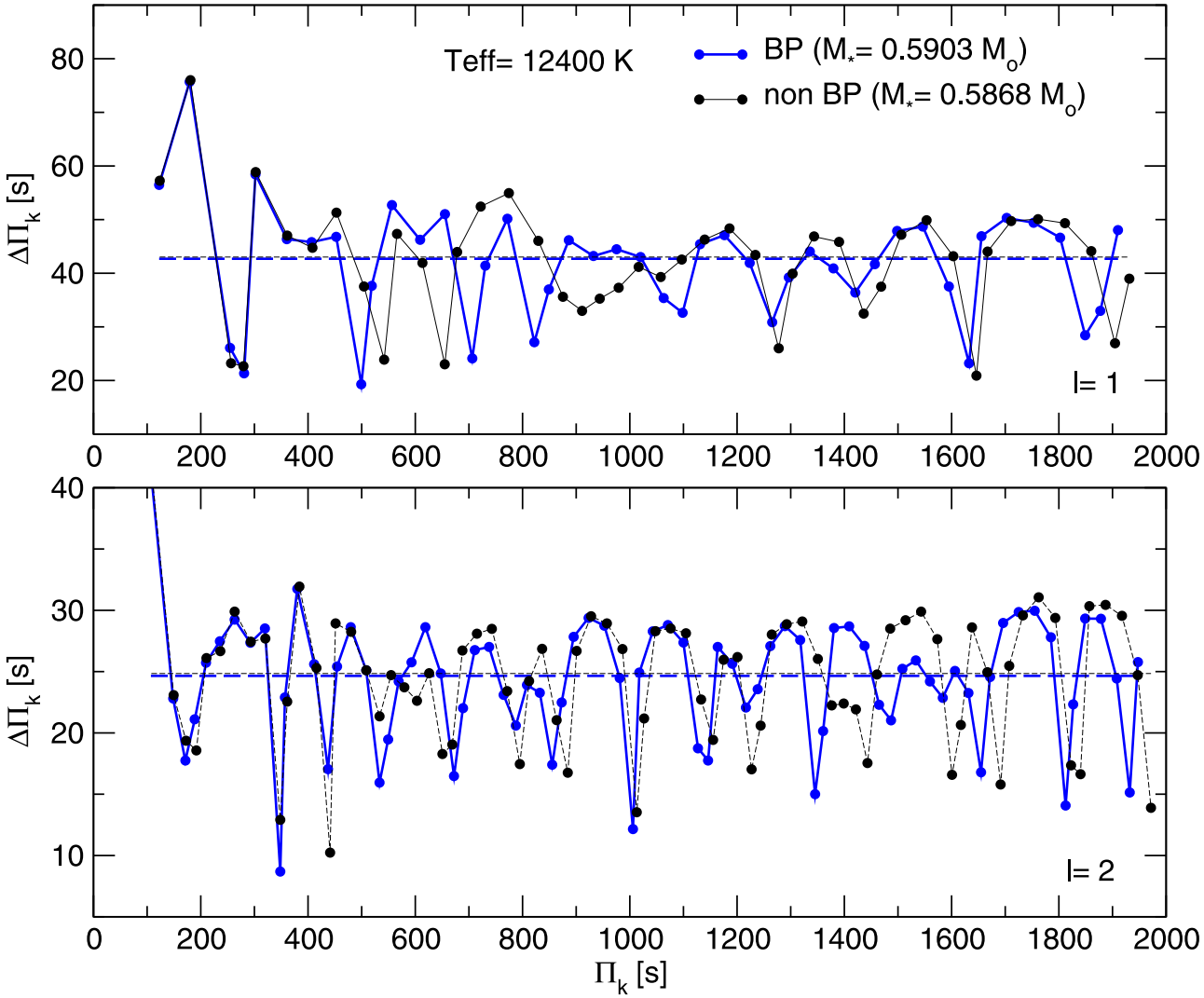

Figure 7. The same as Figure 6, but for ZZ Ceti models with $M_\star = 0.5868 M_\odot$ (non-BP case) and $M_\star = 0.5903 M_\odot$ (BP case).

We have carried out simulations describing the complete evolution of low-mass star progenitors with $Z = 0.01$ evolved from the ZAMS, through the CHeB phase, to the thermal pulses on the AGB, and finally to the domain of the ZZ Ceti stars at advanced stages of WD cooling. We have considered two initial masses at the ZAMS ($M_{\rm ZAMS}/M_\odot = 1.0, 2.5$) taking into account and neglecting the occurrence of BPs during the CHeB phase. We arrive at two important results:

(1) We confirm previous results (e.g., Constantino et al. 2016, 2017) that the occurrence of BPs induces the formation of more massive and ^{16}O-rich cores compared to the case in which BPs have been ignored. At this point, however, we cannot help but notice that the occurrence of BPs is not at all sufficient to explain the excessively large sizes of the WD cores and the anomalously high central ^{16}O abundances predicted by recent asteroseismological studies (Giammichele et al. 2018; Charpinet et al. 2021; Giammichele et al. 2021). However, in line with the finding of these authors, a recent self-consistent implementation of convective penetration during the CHeB phase (Johnston et al. 2023) predicts the formation of larger, ^{16}O-rich WD cores, which would naturally produce more massive remnant C/O cores at the end of He burning. The consequences of convective penetration on the core size and central oxygen abundance of WDs is a topic that deserves to be explored in the future.

(2) Our pulsational analysis indicates that the occurrence of BPs can lead to g-mode periods of ZZ Ceti stars that can differ by up to ∼30 s (excess or defect) compared to the situation in which BPs do not occur during the evolution of the progenitors. It is not surprising that the presence or absence of BPs during the CHeB phase has a significant effect on g-mode periods since Figure 4 shows that there is a clear difference in N^2 between the BP and non-BP cases in the C/O chemical transition at the core. The mean period spacing of pulsating DA WDs is insensitive to the occurrence or not of BPs, while the forward period spacing shows appreciable differences for periods longer than ∼400 s.

We conclude that future seismological period-to-period fits of DAV stars based on evolutionary models generated considering and neglecting the occurrence of BPs during CHeB, could help shed some light on the occurrence of BPs in nature, and a comparable outcome could probably be attained through the analysis of DBV stars.

Acknowledgments

We wish to thank the anonymous referee whose suggestions and comments improved the original version of this work. Part of this work was supported by AGENCIA through the Programa de Modernización Tecnológica BID 1728/OC-AR, and by the PIP 112-200801-00940 grant from CONICET. This research has made use of the NASA Astrophysics Data System.

ORCID iDs

Alejandro H. Córsico https://orcid.org/0000-0002-0006-9900

References

Althaus, L. G., Camisassa, M. E., Miller Bertolami, M. M., Córsico, A. H., & García-Berro, E. 2015, A&A, 576, A9
Althaus, L. G., & Córsico, A. H. 2022, A&A, 663, A167
Althaus, L. G., Córsico, A. H., Bischoff-Kim, A., et al. 2010a, ApJ, 717, 897
Althaus, L. G., Córsico, A. H., Isern, J., & García-Berro, E. 2010b, A&ARv, 18, 471
Althaus, L. G., Serenelli, A. M., Panei, J. A., et al. 2005, A&A, 435, 631
Bell, K. J. 2022, RNAAS, 6, 244
Castellani, V., Chieffi, A., Tornambe, A., & Pulone, L. 1985, ApJ, 296, 204
Charpinet, S., Brassard, P., Giammichele, N., & Fontaine, G. 2019, A&A, 628, L2
Charpinet, S., Giammichele, N., Brassard, P., et al. 2021, arXiv:2107.03797
Constantino, T., Campbell, S. W., & Lattanzio, J. C. 2017, MNRAS, 472, 4900
Constantino, T., Campbell, S. W., Lattanzio, J. C., & van Duijneveldt, A. 2016, MNRAS, 456, 3866
Córsico, A. H., & Althaus, L. G. 2006, A&A, 454, 863
Córsico, A. H., Althaus, L. G., Miller Bertolami, M. M., & Kepler, S. O. 2019, A&ARv, 27, 7
De Gerónimo, F. C., Battich, T., Miller Bertolami, M. M., Althaus, L. G., & Córsico, A. H. 2019, A&A, 630, A100
Fontaine, G., & Brassard, P. 2008, PASP, 120, 1043
Giammichele, N., Charpinet, S., & Brassard, P. 2022, FrASS, 9, 879045
Giammichele, N., Charpinet, S., Fontaine, G., et al. 2018, Natur, 554, 73
Giammichele, N., Charpinet, S., Fontaine, G., et al. 2021, arXiv:2106.15701
Johnston, C., Michielsen, M., Anders, E. H., et al. 2023, arXiv:2312.08315
Kippenhahn, R., Weigert, A., & Weiss, A. 2013, Stellar Structure and Evolution (Berlin: Springer)
Miller Bertolami, M. M. 2016, A&A, 588, A25
Renedo, I., Althaus, L. G., Miller Bertolami, M. M., et al. 2010, ApJ, 717, 183
Salaris, M., Althaus, L. G., & García-Berro, E. 2013, A&A, 555, A96
Salaris, M., Cassisi, S., Pietrinferni, A., Kowalski, P. M., & Isern, J. 2010, ApJ, 716, 1241
Spruit, H. C. 2015, A&A, 582, L2
Sweigart, A. V., & Demarque, P. 1973, in IAU Colloq. 21: Variable Stars in Globular Clusters and in Related Systems, Astrophysics and Space Science Library, ed. J. D. Fernie (Dordrecht: Reidel), 221
Tassoul, M., Fontaine, G., & Winget, D. E. 1990, ApJs, 72, 335
Timmes, F. X., Townsend, R. H. D., Bauer, E. B., et al. 2018, ApJL, 867, L30
Winget, D. E., & Kepler, S. O. 2008, ARA&A, 46, 157
Woosley, S. E., & Heger, A. 2015, ApJ, 810, 34